Ladderane phospholipids form a densely packed membrane with normal hydrazine and anomalously low proton/hydroxide permeability

Frank R. Moss III[a,1], Steven R. Shuken[a,1], Jaron A. M. Mercer[a], Carolyn M. Cohen[a], Thomas M. Weiss[b], Steven G. Boxer[a,2], and Noah Z. Burns[a,2]

[a]Department of Chemistry, Stanford University, Stanford, CA 94305; and [b]Stanford Synchrotron Radiation Laboratory, Stanford Linear Accelerator Center, Stanford University, Menlo Park, CA 94025

Contributed by Steven G. Boxer, July 30, 2018 (sent for review June 24, 2018; reviewed by Erick Carreira and Marjorie Longo)

Ladderane lipids are unique to anaerobic ammonium-oxidizing (anammox) bacteria and are enriched in the membrane of the anammoxosome, an organelle thought to compartmentalize the anammox process, which involves the toxic intermediate hydrazine (N_2H_4). Due to the slow growth rate of anammox bacteria and difficulty of isolating pure ladderane lipids, experimental evidence of the biological function of ladderanes is lacking. We have synthesized two natural and one unnatural ladderane phosphatidylcholine lipids and compared their thermotropic properties in self-assembled bilayers to distinguish between [3]- and [5]-ladderane function. We developed a hydrazine transmembrane diffusion assay using a water-soluble derivative of a hydrazine sensor and determined that ladderane membranes are as permeable to hydrazine as straight-chain lipid bilayers. However, pH equilibration across ladderane membranes occurs 5–10 times more slowly than across straight-chain lipid membranes. Langmuir monolayer analysis and the rates of fluorescence recovery after photobleaching suggest that dense ladderane packing may preclude formation of proton/hydroxide-conducting water wires. These data support the hypothesis that ladderanes prevent the breakdown of the proton motive force rather than blocking hydrazine transmembrane diffusion in anammox bacteria.

ladderane | anammox | lipid bilayer | proton permeability | membrane structure

Lipid membranes are universal features of living systems. Along with membrane proteins, they form the internal and peripheral barriers of cells and organelles and maintain non-equilibrium states necessary for life. Cells produce a diverse array of lipid structures and expend considerable energy to tightly control the lipid compositions of their membranes (1). In conventional phospholipid bilayers, it is known that longer hydrocarbon tails and fewer degrees of unsaturation reduce fluidity and slow lateral diffusion, as well as affecting phase behavior (Fig. 1*A*) (2, 3). However, the physical properties and biological functions of lipids with unconventional structures (*SI Appendix*, Fig. S1) are mostly unexplored.

The ladderane lipids, containing lipid tails terminating in either a [3]-ladderane motif (highlighted in blue in Fig. 1*B*) or a [5]-ladderane motif (highlighted in red in Fig. 1*B*), occur uniquely in anaerobic ammonium-oxidizing (anammox) bacteria and are some of the most structurally exotic lipids known (4–9). Anammox bacteria are not available as a pure culture, and enrichment cultures have doubling times of 1–2 wk (10, 11). Isolation of lipids from anammox enrichment cultures yields a complex and inseparable mixture, preventing biophysical characterization of individual ladderane species (12, 13). To enable experiments on ladderane lipids, we developed de novo enantioselective chemical syntheses of both [3]- and [5]-ladderane lipid tails and ladderane phospholipids (14). We prepared a [5]-ladderane–[3]-ladderane phosphatidylcholine (**[5]\[3]PC**; Fig. 1*B*) and a di-[3]-ladderane phosphatidylcholine (**[3]\[3]PC**; Fig. 1*B*), two of the most common ladderane phospholipids across a range of anammox genera (8). Additionally, we prepared di-[5]-ladderane phosphatidylcholine (**[5]\[5]PC**; Fig. 1*B*), which is not known to occur naturally.

Ladderanes are enriched in the membrane of the anammoxosome, a specialized organelle within which anammox catabolism is thought to occur (4). Ammonium and nitrite are coupled to produce dinitrogen via intermediate hydrazine (N_2H_4); oxidation of hydrazine to dinitrogen is highly exergonic, and this free energy is believed to be harnessed to pump protons across the anammoxosome membrane (15–17). The resulting pH gradient of ∼1 unit in turn powers ATP synthesis (Fig. 1*C*) (18–20). Hydrazine's cellular toxicity and bioenergetic value as a metabolic intermediate have led to the hypothesis that ladderanes serve to prevent the diffusion of hydrazine out of the anammoxosome, thereby protecting the contents of the riboplasm and periplasm from free hydrazine while preserving metabolic energy (4, 20). It has also been reasoned, based on long anammox doubling times and slow hydrazine synthase activity, that ladderanes might prevent the passive diffusion of protons out of the anammoxosome to preserve the proton motive force necessary for ATP synthesis (4, 21). Another theoretical study suggests ladderanes might trap reactive species such as free radicals in addition to protons (22). Although studies on enrichment cultures and lipid extracts suggest

Significance

Ladderane lipids represent exotic natural products containing highly strained, concatenated cyclobutane rings, a motif that has not been found in any other natural products. These lipids are exclusively found in bacteria that carry out anaerobic ammonium oxidation (anammox), suggesting a biological role in the anammox process. The relationship between molecular structure and this metabolism remains unexplored due to a lack of natural lipid material to study. We use an efficient chemical synthesis to create large quantities of pure ladderane lipids for biophysical analysis. This analysis reveals some unusual properties of membranes composed of ladderane lipids. Significantly, ladderane membranes have low proton permeability, which would slow the breakdown of the proton gradient used to synthesize ATP during the slow anammox metabolism.

Author contributions: F.R.M., S.R.S., J.A.M.M., S.G.B., and N.Z.B. designed research; F.R.M., S.R.S., J.A.M.M., C.M.C., and T.M.W. performed research; F.R.M., S.R.S., J.A.M.M., C.M.C., and T.M.W. contributed new reagents/analytic tools; F.R.M., S.R.S., J.A.M.M., T.M.W., S.G.B., and N.Z.B. analyzed data; and F.R.M., S.R.S., S.G.B., and N.Z.B. wrote the paper.

Reviewers: E.C., ETH Zurich; and M.L., University of California, Davis.

The authors declare no conflict of interest.

[1]F.R.M. and S.R.S. contributed equally to this work.

[2]To whom correspondence may be addressed. Email: sboxer@stanford.edu or nburns@stanford.edu.

This article contains supporting information online at www.pnas.org/lookup/suppl/doi:10.1073/pnas.1810706115/-/DCSupplemental.

Published online August 27, 2018.

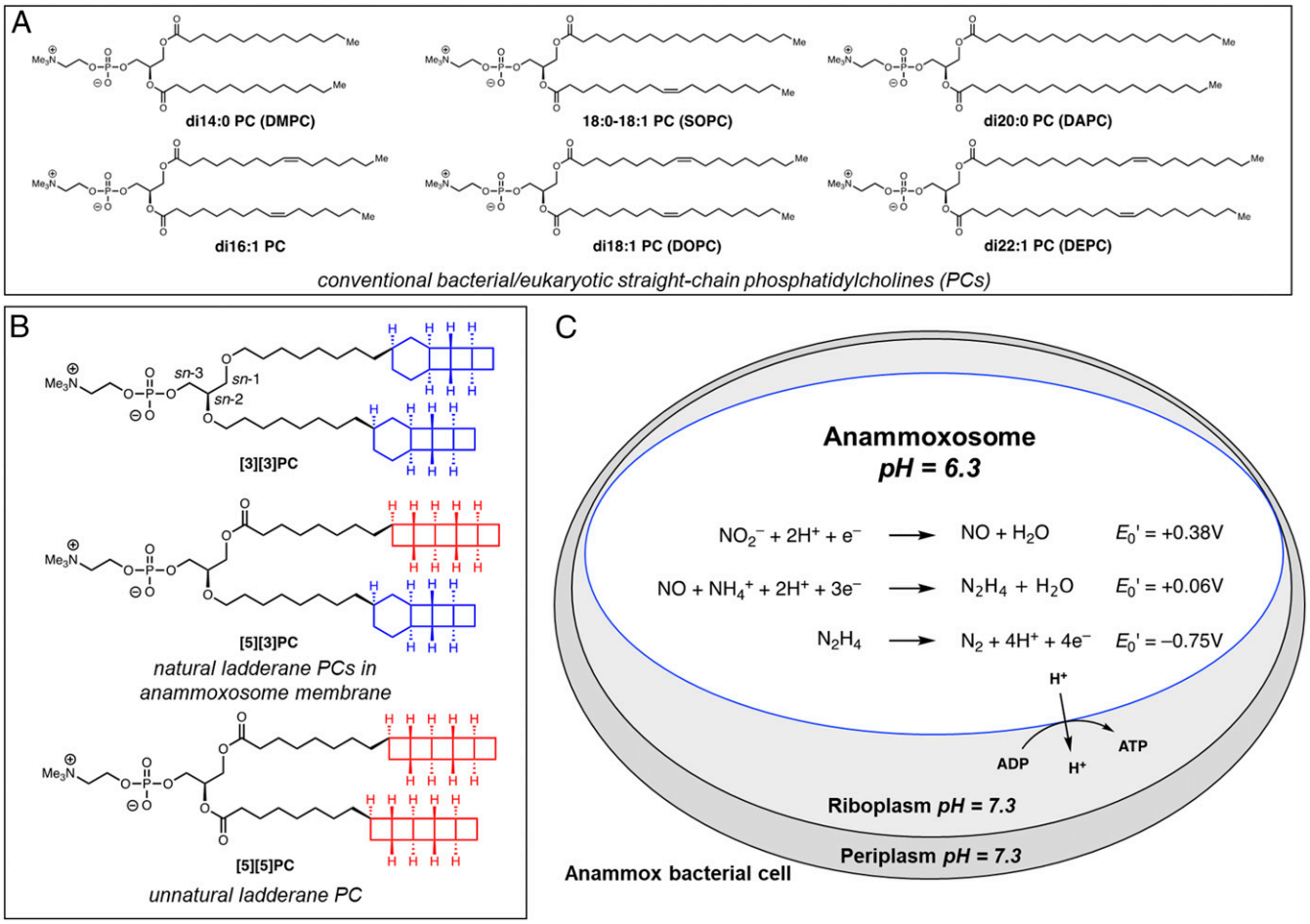

Fig. 1. Lipid structures and anammox metabolism. (*A*) Representative straight-chain PCs. Nomenclature: x:y is a straight chain with x carbons and y degrees of unsaturation. (*B* and *C*) Ladderane lipids such as **[3][3]PC** and **[5][3]PC** occur in the anammoxosome membrane of anammox bacteria. (*B*) **[3][3]PC** and **[5][3]PC** phospholipids and unnatural analog **[5][5]PC** that have been prepared by enantioselective chemical synthesis. (*C*) Anammox catabolism is believed to provide energy to the cell by oxidizing the toxic intermediate hydrazine (N_2H_4). Hydrazine oxidation is thought to be coupled to proton influx, generating a pH gradient that drives ATP synthesis. Standard reduction potentials, E_0', for redox half reactions are shown.

that the anammoxosome membrane is dense and relatively impermeable to dyes, hypotheses about hydrazine and proton permeability remain to be experimentally tested (4, 12). We recently completed the total synthesis of a ladderane phospholipid, which we expand in this work to a total of three phospholipids with distinct tail structures for structure–function studies (14). Biophysical experiments on model membranes composed of these synthetic lipids allow us to identify properties of individual molecular ladderane species.

Results

Syntheses of Ladderane PCs. We recently reported enantioselective total syntheses of a [5]-ladderane fatty acid and a [3]-ladderane fatty alcohol (14). These lipid tails were then elaborated to **[5][3]PC**, **[3][3]PC**, and **[5][5]PC** using a modification of our previously reported phosphatidylcholine synthetic route (*SI Appendix*, Schemes S1–S3).

Differential Scanning Calorimetry. Lipid films were hydrated with a low-melting and high-boiling 1:1 ethylene glycol/phosphate buffer mixture, and differential scanning calorimetry (DSC) was performed to measure the transition temperature (T_m) of the multilamellar lipid dispersions. Control experiments showed that the effect of ethylene glycol on T_m is negligible (*SI Appendix*, Table S1). A single transition between −40 and 80 °C was observed for each ladderane PC. The presence of a [3]-ladderane tail at the *sn*-2 position apparently ensures a low T_m (compare **[5][3]PC**, T_m = 11.8 °C to **[5][5]PC**, T_m = 68.4 °C; Fig. 2*A*). We believe the cyclohexane ring in the [3]-ladderane motif introduces a kink in the lipid tail, mirroring the fluidizing effect of *cis*-unsaturation in the *sn*-2 position tail of a straight-chain lipid [compare 18:0–18:1 PC (SOPC), T_m = 4.1 °C to di18:0 PC (DSPC), T_m = 57.1 °C]; **[5][5]PC** has approximately the same T_m as di20:0 PC (DAPC).

Self-Assembly of Ladderane Phospholipids into Lipid Bilayers. We next evaluated whether ladderane PCs would self- assemble into giant unilamellar vesicles (GUVs) using established methods (23–25). Upon gentle hydration, films of **[3][3]PC** and **[5][3]PC** appeared to form GUVs (Fig. 2 *B* and *C*) with homogeneous incorporation of dye [0.1 mol % Texas Red-DHPE (TR-DHPE)] and spherical shapes confirming that these lipids form fluid bilayers at room temperature. Formation of GUVs from **[5][5]PC** required heating above its T_m, and upon cooling we observed fluorescent objects similar to gel-phase GUVs formed from DAPC (Fig. 2*D* and *SI Appendix*, Fig. S3 *A* and *B*). A 1:1 mixture of **[3][3]PC** and **[5][5]PC** formed GUVs with visible domains that exclude TR-DHPE (Fig. 2*E*) in a manner analogous to mixtures of straight-chain phospholipids that form coexisting phases at room temperature (26). Hydration of **[3][3]PC** or

A Lipid	T_m (°C)
di18:2 PC	-52.7 ± 1.6
di16:1 PC	-33.0 ± 0.1
di18:1 PC (DOPC)	-10.9 ± 0.1
16:0-18:1 PC (POPC)	-4.8 ± 0.1
18:0-18:1 PC (SOPC)	4.1 ± 0.1
di22:1 PC (DEPC)	15.8 ± 0.1
di14:0 PC (DMPC)	24.3 ± 0.1
di18:0 PC (DSPC)	57.1 ± 0.1
di20:0 PC (DAPC)	67.8 ± 0.1
[5][3]PC	11.8 ± 0.2
[3][3]PC	15.2 ± 0.1
[5][5]PC	68.4 ± 0.1

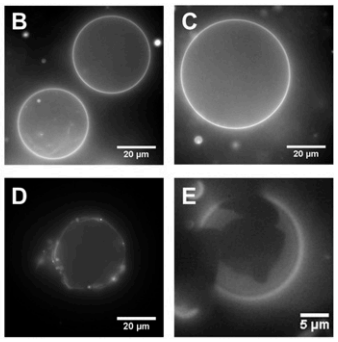

Fig. 2. Transition temperatures and formation of GUVs. (*A*) T_ms of aqueous lamellar dispersions of PCs in 1:1 ethylene glycol/NaH_2PO_4 buffer measured by DSC. (*B–E*) Fluorescence microscope images of GUVs (TR-DHPE or DiI, 0.1 mol %) in 500 mM sucrose. For additional images see *SI Appendix*, Fig. S3. (*B*) **[3][3]PC**, (*C*) **[5][3]PC**, (*D*) **[5][5]PC**, (*E*) 1:1 **[3][3]PC**:**[5][5]PC**.

[5][3]PC films followed by extrusion through a 50-nm-pore polycarbonate membrane resulted in the formation of small unilamellar vesicles (SUVs) (*SI Appendix*, Table S3).

Hydrazine Transmembrane Diffusion Assay. To test the hypothesis that ladderanes form a barrier to transmembrane diffusion of hydrazine, we developed an assay based on a small-molecule sensor that fluoresces upon condensation with hydrazine (27). We prepared a derivative with added hydrophilic sulfonate and amide groups to improve aqueous solubility and presumably reduce interactions between the dye and the membrane (*SI Appendix*, Figs. S4–S11 and Schemes S4–S6); the final hydrazine sensor (**HS**)-based hydrazine transmembrane diffusion kinetic assay design is illustrated in Fig. 3*A* (28). We also confirmed that HS does not localize in lipid bilayers (*SI Appendix*, section 9).

We performed this hydrazine diffusion assay on SUVs composed of several straight-chain PCs, **[3][3]PC**, and **[5][3]PC**. SUVs encapsulating **HS** in a pH = 7.4 phosphate buffer were added to an equiosmolar pH = 7.4 buffer containing hydrazine, and changes in the fluorescence intensity were measured (Fig. 3*B*). Among straight-chain PCs, hydrazine transmembrane diffusion rates depended strongly on hydrophobic tail length (Fig. 3*C*), likely due to different bilayer thicknesses among these lipids (29–31). SUVs of ladderane PCs exhibited half-lives ($t_{1/2}$s) of hydrazine transmembrane diffusion well within the range exhibited by SUVs of straight-chain PCs. We have also conducted this diffusion assay at the anammoxosome-relevant pH of 6.3 with SOPC, di22:1 PC (DEPC), and **[3][3]PC**. Transmembrane diffusion rates are all slower, as expected, but maintain the same trend as at pH = 7.4 (*SI Appendix*, section 10).

Small-Angle X-Ray Scattering. To examine the relationship between hydrazine diffusion rate and bilayer thickness, we performed small angle X-ray scattering (SAXS) on rigorously extruded SUVs of unsaturated straight-chain PCs and ladderane PCs (Fig. 3*C*). Bilayers of straight-chain PCs increased in thickness with increasing chain length from 3.25 nm for di16:1 PC to 4.37 nm for di22:1 PC. The [3]-ladderane and [5]-ladderane tails in our synthetic ladderane phospholipids each contain 20 carbons, and **[3][3]PC** and **[5][3]PC** formed bilayers of about the same thickness as di20:1 PC (~4 nm). SAXS curves also confirmed the high level of unilamellarity of SUVs (see discussion in *SI Appendix*, section 12).

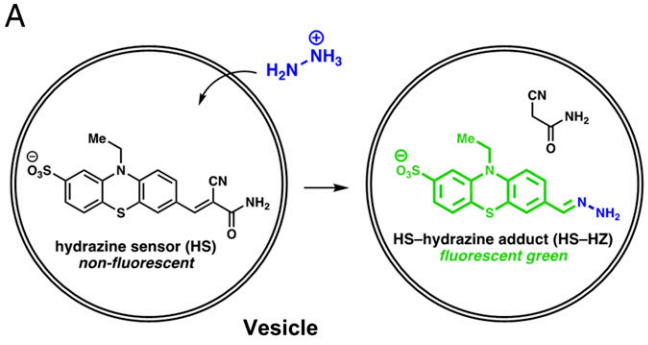

C Lipid	N_2H_4 Diff. $t_{1/2}$ (min)	Bilayer Thickness (nm)
di18:2 PC	23.0 ± 0.9	--
di16:1 PC	23.0 ± 2.7	3.25 ± 0.004
di18:1 PC (DOPC)	54.4 ± 5.6	3.53 ± 0.006
18:0-18:1 PC (SOPC)	50.5 ± 0.5	--
di20:1 PC	--	3.96 ± 0.005
di22:1 PC (DEPC)	98.9 ± 6.0	4.37 ± 0.004
[5][3]PC	47.4 ± 0.9	3.98 ± 0.008
[3][3]PC	71.5 ± 2.0	4.00 ± 0.007

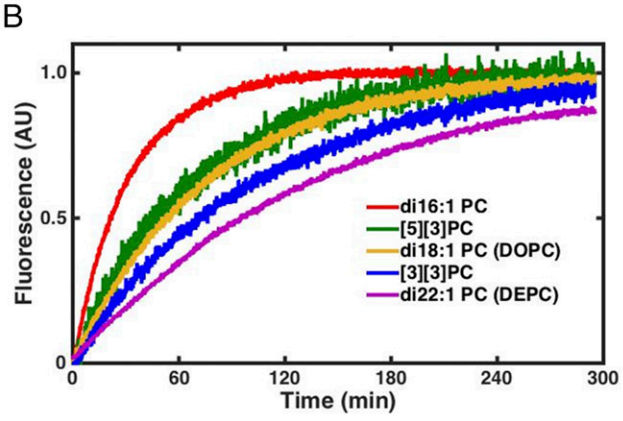

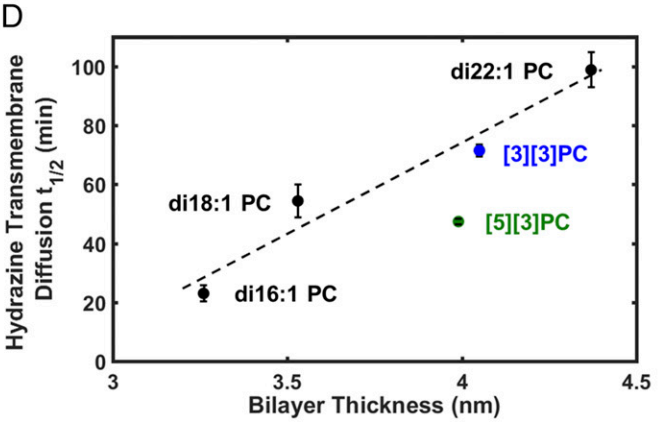

Fig. 3. Hydrazine transmembrane diffusion assay and bilayer thickness as estimated by SAXS. (*A*) Illustration of N_2H_4 transmembrane diffusion assay using a water-soluble derivative (**HS**) of a fluorogenic hydrazine sensor. (*B*) Hydrazine transmembrane diffusion curves for representative straight-chain and ladderane PCs. (*C*) Table of hydrazine transmembrane diffusion half-lives and bilayer thicknesses. (*D*) Hydrazine transmembrane diffusion half-life vs. bilayer thickness. Dashed line illustrates linear correlation for di16:1 PC, di18:1 PC, di22:1 PC, and **[3][3]PC**.

pH Equilibration Across Membranes. To test the hypothesis that ladderanes form a barrier to transmembrane diffusion of protons/hydroxide ions, we performed a carboxyfluorescein (CF)-based assay of pH equilibration (Fig. 4*A*) on SUVs of several straight-chain PCs, **[3][3]PC**, and **[5][3]PC** (32). SUVs encapsulating CF at pH = 7.2 in bis-Tris propane buffer were added to equiosmolar pH = 5.8 bis-Tris propane buffer, creating a transmembrane pH gradient that spontaneously decayed over time. The decrease in CF fluorescence was used to monitor the decrease in pH inside the SUVs as protons/hydroxide ions equilibrated across the bilayers. We also performed control experiments with valinomycin to confirm that a buildup of membrane potential was not affecting relative pH equilibration rates and with gramicidin to confirm that vesicles were unilamellar. We confirmed that valinomycin inserts into ladderane bilayers with the fluorescent K^+ sensor PBFI (*SI Appendix*, section 13) (33). Equilibration of pH across **[3][3]PC** and **[5][3]PC** bilayers was approximately an order of magnitude slower than across membranes composed of straight-chain PCs (48–75 min vs. 0.33–6.9 min $t_{1/2}$) (Fig. 4 *B* and *C*). We observe a correlation between T_m and pH equilibration $t_{1/2}$ for straight-chain PCs; however, **[5][3]PC** and **[3][3]PC** deviate from this trend, suggesting that unique intermolecular interactions between ladderane lipid tails affect rates of pH equilibration (Fig. 4*D*). These interactions remain present in a mixture of **[3][3]PC** with 16:0–18:1 PC (POPC) as indicated by a pH equilibration $t_{1/2}$ of 31 min (*SI Appendix*, section 13).

Pressure-Area Isotherms of Langmuir Monolayers. To help explain the low proton/hydroxide permeability of ladderane PC bilayers, we investigated the physical properties of PC monolayers at the air–water interface. Ladderane PC monolayers collapse at surface pressures similar to liquid-phase monolayers of POPC (Fig. 5*A*), yet their compressibilities, *C*, are similar to those of solid-phase monolayers of DAPC (Fig. 5*C*). In addition, monolayers of ladderane phospholipids have mean molecular areas (MMAs) smaller than fluid straight-chain PCs (Fig. 5*C*). These data suggest that at room temperature the ladderane PC monolayers exist in a phase that is fluid but more tightly packed than straight-chain PCs. Pressure-area isotherms for **[5][3]PC** and **[3][3]PC** are qualitatively similar to the previously published isotherm for a ladderane PC extract (12).

Fluorescence Recovery After Photobleaching. To quantitate fluidity in ladderane PC bilayers, we performed fluorescence recovery after photobleaching (FRAP) experiments on glass-supported lipid bilayers (SLBs) using Oregon Green-DHPE (OG-DHPE) as a fluorescent probe (Fig. 5*B*). As expected for lipids in a gel phase at room temperature, SLBs of **[5][5]PC** showed no lateral diffusion (Fig. 5*B*). SLBs of **[5][3]PC** and **[3][3]PC** exhibited lateral diffusion coefficients, *D*, at least one order of magnitude lower than SLBs of straight-chain PCs (0.24–0.29 $\mu m^2/s$ vs. 2.73–3.93 $\mu m^2/s$) (Fig. 5 *B* and *C*). Straight-chain PCs show a linear correlation between *D* and T_m while ladderane PCs deviate from this trend (Fig. 5*D*).

Discussion and Conclusions

The facile preparation of vesicles, monolayers, and supported bilayers of **[3][3]PC** and **[5][3]PC** was not anticipated, as their

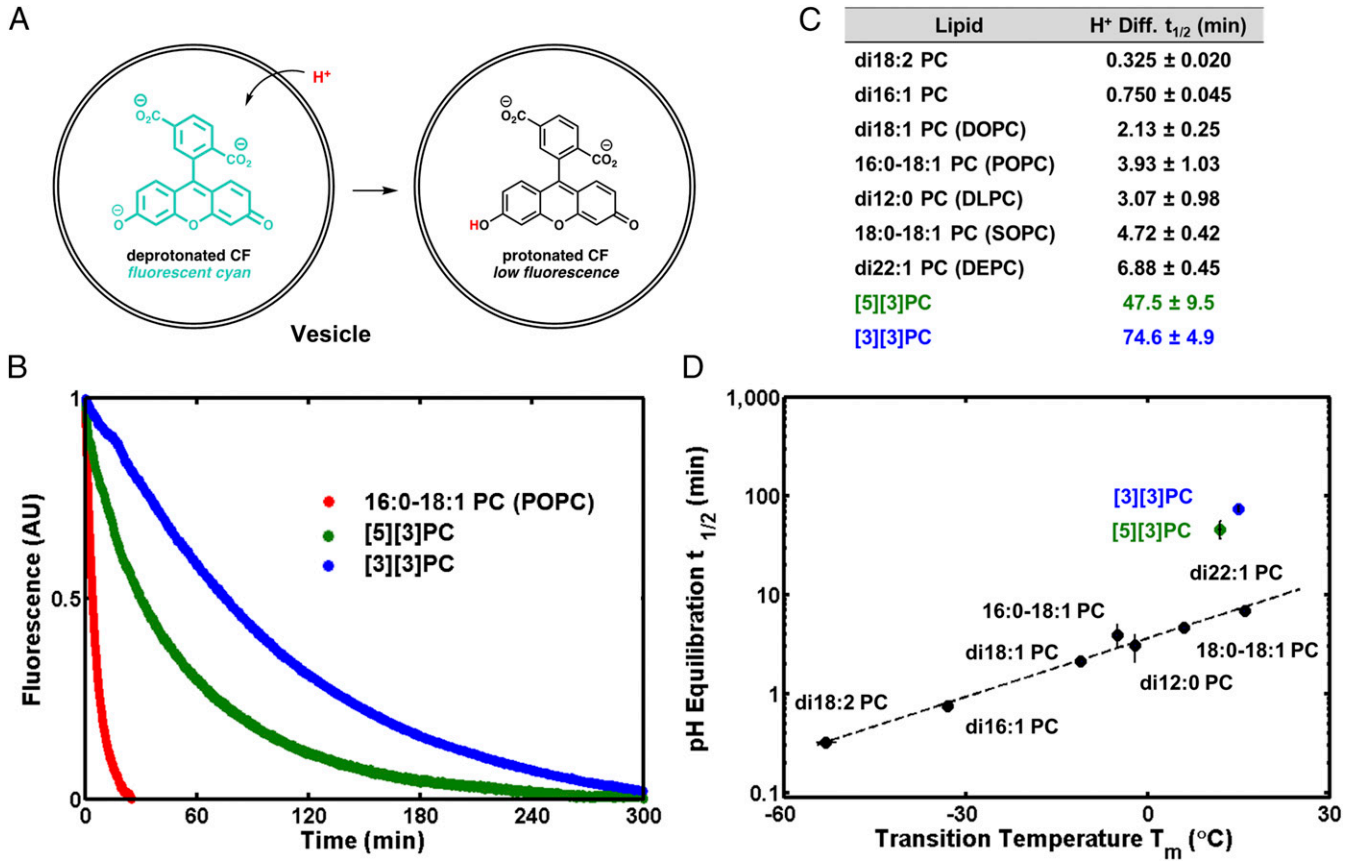

Lipid	H^+ Diff. $t_{1/2}$ (min)
di18:2 PC	0.325 ± 0.020
di16:1 PC	0.750 ± 0.045
di18:1 PC (DOPC)	2.13 ± 0.25
16:0-18:1 PC (POPC)	3.93 ± 1.03
di12:0 PC (DLPC)	3.07 ± 0.98
18:0-18:1 PC (SOPC)	4.72 ± 0.42
di22:1 PC (DEPC)	6.88 ± 0.45
[5][3]PC	47.5 ± 9.5
[3][3]PC	74.6 ± 4.9

Fig. 4. pH equilibration assay. (*A*) Illustration of assay: influx of protons into (or efflux of hydroxide from) vesicles results in the protonation of CF and a decrease in fluorescence intensity. (*B*) Kinetic curves show that equilibration of pH across ladderane PC bilayers is much slower than across straight-chain PC bilayers, as illustrated by the case of POPC. (*C*) Table of pH equilibration half-lives $t_{1/2}$. (*D*) The logarithm of pH equilibration $t_{1/2}$ and straight-chain PC T_m are correlated, while ladderane PCs deviate from this trend.

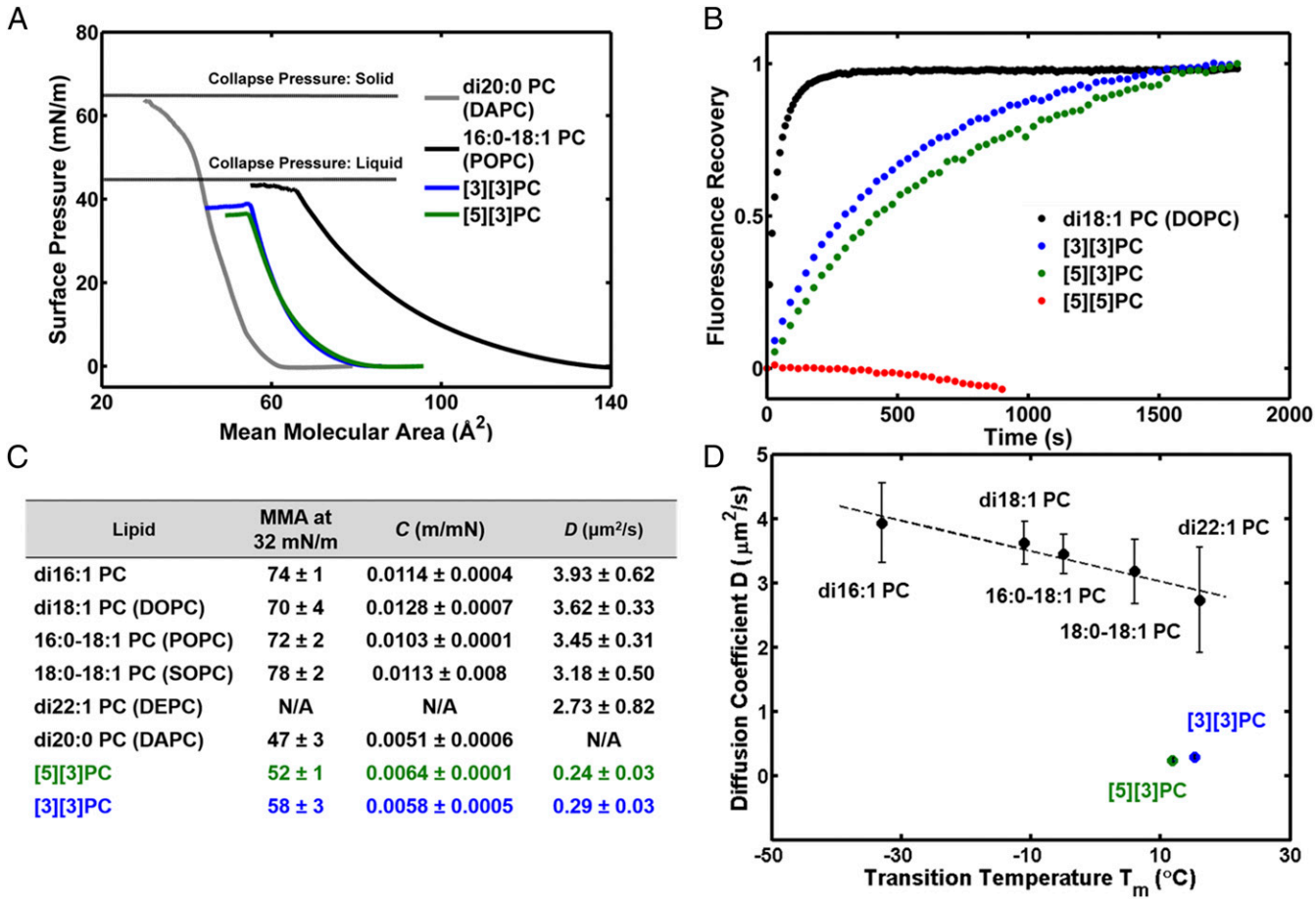

C

Lipid	MMA at 32 mN/m	*C* (m/mN)	*D* (μm²/s)
di16:1 PC	74 ± 1	0.0114 ± 0.0004	3.93 ± 0.62
di18:1 PC (DOPC)	70 ± 4	0.0128 ± 0.0007	3.62 ± 0.33
16:0-18:1 PC (POPC)	72 ± 2	0.0103 ± 0.0001	3.45 ± 0.31
18:0-18:1 PC (SOPC)	78 ± 2	0.0113 ± 0.008	3.18 ± 0.50
di22:1 PC (DEPC)	N/A	N/A	2.73 ± 0.82
di20:0 PC (DAPC)	47 ± 3	0.0051 ± 0.0006	N/A
[5][3]PC	52 ± 1	0.0064 ± 0.0001	0.24 ± 0.03
[3][3]PC	58 ± 3	0.0058 ± 0.0005	0.29 ± 0.03

Fig. 5. Biophysical studies on PC monolayers and bilayers. (*A*) Pressure-area isotherms of Langmuir monolayers composed of di20:0 PC (DAPC, T_m = 68 °C), 16:0–18:1 PC (POPC, T_m = −4.8 °C), and ladderane PCs (T_m = 12–15 °C). (*B*) FRAP curves of ladderane PCs and a representative straight-chain PC, di18:1 PC (DOPC). (*C*) Physical parameters extracted from isotherms and FRAP curves. MMA is given in square angstroms. N/A, not assessed. (*D*) *D* correlates linearly with T_m for straight-chain PCs, but ladderane PCs deviate from this trend.

unique structural elements might be expected to alter their molecular spontaneous curvature and favor nonbilayer structures. However, self-assembly is consistent with the observation that ladderanes are the primary lipid components of the membranes in anammox bacteria, suggesting a major structural role for ladderane phospholipids. Anammox bacteria rely on a pH gradient to drive ATP synthesis (19, 20). Loss of this pH gradient during the slow anammox metabolism would make this process unviable as a source of energy for the cell. Our data support the hypothesis that ladderanes evolved at least in part to impede the loss of this vital pH gradient. Our biophysical results are qualitatively similar to results from complex mixtures of ladderanes, but we are able to observe functional distinctions between individual molecules that are lost in mixtures (for a discussion see *SI Appendix*, section 16) (12, 13). We note that this study was enabled by the success of a scalable natural product total synthesis (14).

Although much work has been done to understand the permeability of membranes to easily detectable drugs and organic dyes, methods of quantifying transmembrane diffusion of small hydrophilic molecules such as hydrazine in real time are limited, often to indirect assays (34–36). The lack of correlation between the rates of pH equilibration and hydrazine transmembrane diffusion provides experimental evidence that these processes occur by different mechanisms. Evidence from the literature supports a model in which proton/hydroxide diffusion occurs via water molecules in the bilayer that act as proton wires or water clusters that carry protons (30, 37–40). Transmembrane diffusion of other ions (e.g., K^+) and small neutral molecules (e.g., H_2O, O_2, and CO_2), the rates of which are directly dependent on bilayer thickness, is thought to occur via direct partitioning into the bilayer and diffusion through the hydrophobic region of the bilayer (21, 41). Our data are consistent with the idea that this is the case for hydrazine. Our data do not support the hypothesis that ladderane PCs alone offer any advantage with respect to hydrazine permeability. Ladderane PC bilayers and straight-chain PC bilayers have similar rates of hydrazine transmembrane diffusion. Notably, the relative hydrazine permeability of ladderane bilayers compared with conventional PC bilayers was correctly predicted by molecular dynamics simulations (42). Hydrazine containment by other means, such as rapid conversion within the hydrazine synthase complex or retention within encapsulin nanocompartments, remains a possibility (17, 43).

In contrast, equilibration of pH across the **[3][3]PC** bilayer was at least 10 times slower than across bilayers composed of any straight-chain PC. To the best of our knowledge this is the slowest known pH equilibration to be measured across a homogeneous PC bilayer; interestingly, very slow pH equilibration across archaea-inspired tetraether lipid monolayers is also known (33). Rates of pH equilibration for straight-chain PC bilayers correlate with their T_ms, which reflect the strength of intermolecular interactions and lipid packing. Our data are consistent with a model in which water must disrupt lipid–lipid interactions to form a proton-conductive wire or cluster in the hydrophobic region of the bilayer. For straight-chain PCs these interactions are accurately reflected in the T_ms, but this

correlation breaks down with **[3][3]PC** and **[5][3]PC**. Monolayers of **[3][3]PC** and **[5][3]PC** at room temperature have smaller MMAs and lower compressibilities than fluid straight-chain PC monolayers, suggesting tighter packing and a higher level of molecular order in the fluid bilayer that is somehow not reflected in the T_m. However, these stronger intermolecular interactions are reflected in the slower lateral diffusion rates in SLBs. Finally, it is interesting to note that **[3][3]PC** and **[5][3]PC**, which both have 20-carbon ladderane tails, form bilayers of similar thickness to di20:1 PC, indicating that the conformational rigidity of the polycyclobutane ladderane motifs counterbalances their shortened structure for a null net effect on bilayer thickness.

Strong London dispersion interactions between ladderane hydrocarbons have been predicted computationally (44). The strong ladderane–ladderane interactions might resist the formation of a proton-conductive water cluster/wire, which would disrupt these interactions (35, 39, 41, 42). This is consistent with the very low D of ladderane bilayers, as this same disruption of packing is necessary for the OG-DHPE to diffuse laterally. D correlates well with pH equilibration $t_{1/2}$ for all PCs assessed, including ladderanes, indicating that D reports on the strength of the physical interactions relevant to proton/hydroxide permeability (*SI Appendix*, Fig. S22). Hydrazine, which is much smaller than a water cluster, may be able to diffuse through small, transient spaces without wholly disrupting ladderane–ladderane packing (12, 45). More generally, we have demonstrated that lipid packing in the hydrophobic region of the lipid bilayer can strongly affect the permeability of the bilayer to small ions. Cells may utilize this mechanism to control the permeabilities of their membranes.

ACKNOWLEDGMENTS. We thank Dr. Stephen R. Lynch for assistance with NMR spectroscopy and Katherine N. Liu for assistance in the development of the hydrazine transmembrane diffusion assay. This work was supported by Stanford University, the Terman Foundation, National Institutes of Health Grants GM069630 and GM118044 (to S.G.B.), the NSF Biophysics Program (S.G.B.), the National Science Foundation (graduate fellowships to J.A.M.M., C.M.C., and S.R.S.), and the Center for Molecular Analysis and Design (graduate fellowship to F.R.M.). Use of the Stanford Synchrotron Radiation Lightsource (SSRL), SLAC National Accelerator Laboratory, is supported by the US Department of Energy (DOE), Office of Science, Office of Basic Energy Sciences under Contract DE-AC02-76SF00515. The SSRL Structural Molecular Biology Program is supported by the DOE Office of Biological and Environmental Research and by the National Institutes of Health, National Institute of General Medical Sciences (NIGMS) (including P41GM103393). The contents of this publication are solely the responsibility of the authors and do not necessarily represent the official views of NIGMS or NIH. Part of this work was performed at the Stanford Nano Shared Facilities, supported by the NSF under Award ECCS-1542152.

1. van Meer G, Voelker DR, Feigenson GW (2008) Membrane lipids: Where they are and how they behave. *Nat Rev Mol Cell Biol* 9:112–124.
2. Alberts B, et al. (2008) Membrane structure. *Molecular Biology of the Cell* (Garland, New York), pp 617–650.
3. Simons K, Vaz WLC (2004) Model systems, lipid rafts, and cell membranes. *Annu Rev Biophys Biomol Struct* 33:269–295.
4. Sinninghe Damsté JS, et al. (2002) Linearly concatenated cyclobutane lipids form a dense bacterial membrane. *Nature* 419:708–712.
5. Nouri DH, Tantillo DJ (2006) They came from the deep: Syntheses, applications, and biology of ladderanes. *Curr Org Chem* 10:2055–2075.
6. Sinninghe Damsté JS, Rijpstra WIC, Geenevasen JAJ, Strous M, Jetten MSM (2005) Structural identification of ladderane and other membrane lipids of planctomycetes capable of anaerobic ammonium oxidation (anammox). *FEBS J* 272:4270–4283.
7. Boumann HA, et al. (2006) Ladderane phospholipids in anammox bacteria comprise phosphocholine and phosphoethanolamine headgroups. *FEMS Microbiol Lett* 258:297–304.
8. Rattray JE, et al. (2008) Ladderane lipid distribution in four genera of anammox bacteria. *Arch Microbiol* 190:51–66.
9. Sinninghe Damsté JS, et al. (2004) A mixed ladderane/*n*-alkyl glycerol diether membrane lipid in an anaerobic ammonium-oxidizing bacterium. *Chem Commun (Camb)*, 2590–2591.
10. Strous M, Heijnen JJ, Kuenen JG, Jetten MSM (1998) The sequencing batch reactor as a powerful tool for the study of slowly growing anaerobic ammonium-oxidizing microorganisms. *Appl Microbiol Biotechnol* 50:589–596.
11. van der Star WRL, et al. (2008) The membrane bioreactor: A novel tool to grow anammox bacteria as free cells. *Biotechnol Bioeng* 101:286–294.
12. Boumann HA, et al. (2009) Biophysical properties of membrane lipids of anammox bacteria: I. Ladderane phospholipids form highly organized fluid membranes. *Biochim Biophys Acta* 1788:1444–1451.
13. Boumann HA, et al. (2009) Biophysical properties of membrane lipids of anammox bacteria: II. Impact of temperature and bacteriohopanoids. *Biochim Biophys Acta* 1788:1452–1457.
14. Mercer JAM, et al. (2016) Chemical synthesis and self-assembly of a ladderane phospholipid. *J Am Chem Soc* 138:15845–15848.
15. Kuenen JG (2008) Anammox bacteria: From discovery to application. *Nat Rev Microbiol* 6:320–326.
16. Kartal B, et al. (2011) Molecular mechanism of anaerobic ammonium oxidation. *Nature* 479:127–130.
17. Dietl A, et al. (2015) The inner workings of the hydrazine synthase multiprotein complex. *Nature* 527:394–397.
18. van der Star WRL, et al. (2010) An intracellular pH gradient in the anammox bacterium *Kuenenia stuttgartiensis* as evaluated by 31P NMR. *Appl Microbiol Biotechnol* 86:311–317.
19. van Niftrik LA, et al. (2004) The anammoxosome: An intracytoplasmic compartment in anammox bacteria. *FEMS Microbiol Lett* 233:7–13.
20. Kartal B, et al. (2013) How to make a living from anaerobic ammonium oxidation. *FEMS Microbiol Rev* 37:428–461.
21. Jetten MSM, et al. (2009) Biochemistry and molecular biology of anammox bacteria. *Crit Rev Biochem Mol Biol* 44:65–84.
22. Nouri DH, Tantillo DJ (2012) Attack of radicals and protons on ladderane lipids: Quantum chemical calculations and biological implications. *Org Biomol Chem* 10: 5514–5517.
23. Reeves JP, Dowben RM (1969) Formation and properties of thin-walled phospholipid vesicles. *J Cell Physiol* 73:49–60.
24. Walde P, Cosentino K, Engel H, Stano P (2010) Giant vesicles: Preparations and applications. *ChemBioChem* 11:848–865.
25. Akashi K, Miyata H, Itoh H, Kinosita K, Jr (1996) Preparation of giant liposomes in physiological conditions and their characterization under an optical microscope. *Biophys J* 71:3242–3250.
26. Veatch SL, Keller SL (2003) Separation of liquid phases in giant vesicles of ternary mixtures of phospholipids and cholesterol. *Biophys J* 85:3074–3083.
27. Sun M, Guo J, Yang Q, Xiao N, Li Y (2014) A new fluorescent and colorimetric sensor for hydrazine and its application in biological systems. *J Mater Chem B* 2:1846–1851.
28. Hughes LD, Rawle RJ, Boxer SG (2014) Choose your label wisely: Water-soluble fluorophores often interact with lipid bilayers. *PLoS One* 9:e87649.
29. Walter A, Gutknecht J (1986) Permeability of small nonelectrolytes through lipid bilayer membranes. *J Membr Biol* 90:207–217.
30. Lorent JH, Levental I (2015) Structural determinants of protein partitioning into ordered membrane domains and lipid rafts. *Chem Phys Lipids* 192:23–32.
31. Pignataro MF, et al. (2015) Modulation of plasma membrane Ca^{2+}-ATPase by neutral phospholipids: Effect of the micelle-vesicle transition and the bilayer thickness. *J Biol Chem* 290:6179–6190.
32. Koyanagi T, et al. (2016) Cyclohexane rings reduce membrane permeability to small ions in archaea-inspired tetraether lipids. *Angew Chem Int Ed Engl* 55:1890–1893.
33. Hervé M, Cybulska B, Gary-Bobo CM (1985) Cation permeability induced by valinomycin, gramicidin D and amphotericin B in large lipidic unilamellar vesicles studied by ^{31}P-NMR. *Eur Biophys J* 12:121–128.
34. Liu H, et al. (2003) *In vitro* permeability of poorly aqueous soluble compounds using different solubilizers in the PAMPA assay with liquid chromatography/mass spectrometry detection. *Pharm Res* 20:1820–1826.
35. Bangham AD, Standish MM, Watkins JC (1965) Diffusion of univalent ions across the lamellae of swollen phospholipids. *J Mol Biol* 13:238–252.
36. Mathai JC, Sprott GD, Zeidel ML (2001) Molecular mechanisms of water and solute transport across archaebacterial lipid membranes. *J Biol Chem* 276:27266–27271.
37. Paula S, Deamer DW (1999) Membrane permeability barriers to ionic and polar solutes. *Curr Top Membr* 48:77–95.
38. Deamer DW, Nichols JW (1989) Proton flux mechanisms in model and biological membranes. *J Membr Biol* 107:91–103.
39. Marrink SJ, Jähnig F, Berendsen HJC (1996) Proton transport across transient single-file water pores in a lipid membrane studied by molecular dynamics simulations. *Biophys J* 71:632–647.
40. Tepper HL, Voth GA (2005) Protons may leak through pure lipid bilayers via a concerted mechanism. *Biophys J* 88:3095–3108.
41. Mathai JC, Tristram-Nagle S, Nagle JF, Zeidel ML (2008) Structural determinants of water permeability through the lipid membrane. *J Gen Physiol* 131:69–76.
42. Chaban VV, Nielsen MB, Kopec W, Khandelia H (2014) Insights into the role of cyclic ladderane lipids in bacteria from computer simulations. *Chem Phys Lipids* 181:76–82.
43. Giessen TW, Silver PA (2017) Widespread distribution of encapsulin nanocompartments reveals functional diversity. *Nat Microbiol* 2:17029.
44. Wagner JP, Schreiner PR (2014) Nature utilizes unusual high London dispersion interactions for compact membranes composed of molecular ladders. *J Chem Theory Comput* 10:1353–1358.
45. Paula S, Volkov AG, Van Hoek AN, Haines TH, Deamer DW (1996) Permeation of protons, potassium ions, and small polar molecules through phospholipid bilayers as a function of membrane thickness. *Biophys J* 70:339–348.